Enhanced exchange bias coupling in Fe/Fe$_x$Mn$_{1-x}$ bilayer by reducing vertical lattice constants

Wen-Chin Lin, Bo-Yao Wang, Te-Yu Chen, Ling-Chih Lin, and Yu-Wen Liao
Department of Physics, National Taiwan University, 10617 Taipei, Taiwan
and Institute of Atomic and Molecular Sciences, Academia Sinica, 10617 Taipei, Taiwan

Wei Pan
Department of Physics, National Taiwan University, 10617 Taipei, Taiwan
and Department of Physics, National Chung Cheng University, Min-Hsiung Chia-Yi 62102, Taiwan

Nai-Yeou Jih
Department of Physics, National Taiwan University, 10617 Taipei, Taiwan

Ker-Jar Song
Institute of Atomic and Molecular Sciences, Academia Sinica, 10617 Taipei, Taiwan

Minn-Tsong Lin[a)]
Department of Physics, National Taiwan University, 10617 Taipei, Taiwan
and Institute of Atomic and Molecular Sciences, Academia Sinica, 10617 Taipei, Taiwan

The modification of crystalline structure by epitaxial growth on different single crystals induces crucial effects on the exchange bias coupling. Due to the larger lattice constant (a_0) of Cu$_3$Au(100) ($a_0 = 3.75$ Å), the vertical lattice constants of Fe/Fe$_x$Mn$_{1-x}$ films on Cu$_3$Au(100) are much smaller than those of the Fe/Fe$_x$Mn$_{1-x}$/Cu(100) system (Cu: $a_0 = 3.61$ Å). By reducing the vertical lattice constants, the interface exchange bias coupling energy of Fe/Fe$_x$Mn$_{1-x}$/Cu$_3$Au(100) is enhanced to be 0.12–0.18 erg/cm^2, which is approximately four times that of the Cu(100) system. © *2007 American Institute of Physics.* [DOI: 10.1063/1.2435514]

Due to the application of magnetoresistance in memory recording, read sensor, etc., many studies[1] about the various exchange bias systems have been performed in the last decade. Basically the exchange bias systems are composed of ferromagnetic (FM) and antiferromagnetic (AFM) layers. After a field-cooling process, the exchange coupling between FM and AFM layers induces a unidirectional anisotropy. Thus a shift from the zero field position of the hysteresis loop for FM layer, the so-called exchange bias field (H_e), as well as the enhanced coercivity (H_c) usually can be observed.[1]

From the application's point of view, how to advance the H_e in an exchange bias system is an important issue. The physical factors to promote the exchange bias coupling are also of fundamental interests. For example, in many previous studies,[1] the high temperature annealing is used to increase H_e. The annealing process usually induces alloy interdiffusion and structural transition at the FM/AFM interface. Most of the reports are largely empirical and the physics is also quite complicated.[1] Usually, the epitaxial growth of single-crystalline metallic FM film on metallic AFM Mn alloy may simplify the physical conditions and then it will be possible to characterize or manipulate the FM/AFM coupling in more detail. In this letter, single-crystalline AFM Fe$_x$Mn$_{1-x}$ alloy films are used to detect the structural effect on the exchange bias coupling. Several previous reports are already focused on the structural and magnetic properties of single-crystalline Fe$_x$Mn$_{1-x}$ thin films on Cu(100) because of the small lattice mismatch.[2–9] We tune the crystalline structure of the FM/AFM layers through the epitaxial growth on different sub-

strates of Cu$_3$Au(100) and Cu(100) with the lattice constants of 3.75 and 3.61 Å, respectively. In Fig. 1 the lattice mismatch between Cu, Cu$_3$Au, and Fe$_x$Mn$_{1-x}$ bulk alloy is shown as functions of the Fe concentration x.[10] Since the lattice constant of the bulk Fe$_x$Mn$_{1-x}$ alloy is right between those of the Cu and Cu$_3$Au, Fe$_x$Mn$_{1-x}$ films can be grown on Cu(100) and Cu$_3$Au(100) with different strain directions, which may cause expanded and suppressed vertical lattice constants ($d_\perp$), respectively. By reducing the vertical lattice constants, the interface exchange bias coupling energy of Fe/Fe$_x$Mn$_{1-x}$/Cu$_3$Au(100) is enhanced to be 0.12–0.18 erg/cm^2, which is approximately four times that of the Cu(100) system.
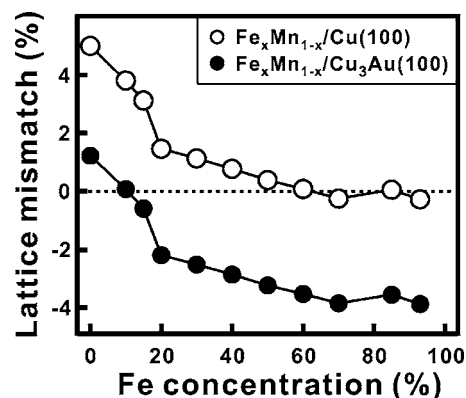

FIG. 1. Lattice mismatch of Fe$_x$Mn$_{1-x}$/Cu(100) and Fe$_x$Mn$_{1-x}$/Cu$_3$Au(100) systems shown as functions of Fe concentration x (Refs. 2 and 10). The lattice mismatch is calculated by the definition $(a_f - a_s)/a_s$, where a_f and a_s are the lattice constants of the bulk Fe$_x$Mn$_{1-x}$ (Ref. 10) and the substrate.

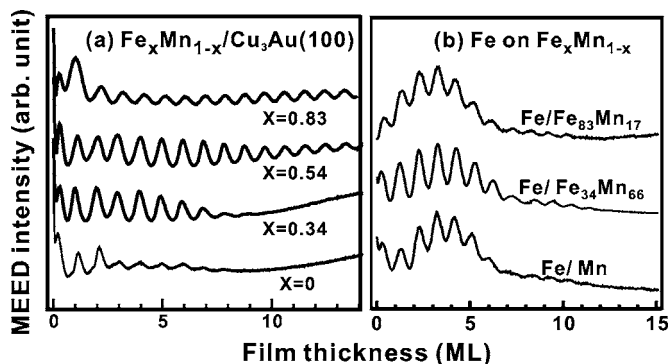a)Electronic mail: mtlin@phys.ntu.edu.tw

FIG. 2. (a) MEED oscillation curves of various Fe_xMn_{1-x} films grown on $Cu_3Au(100)$ at RT. (b) MEED curves of Fe films grown on 15 ML $Fe_xMn_{1-x}/Cu_3Au(100)$ at RT.

FIG. 4. (Color online) (a) Vertical lattice constants of 17 ML $Fe_xMn_{1-x}/Cu(100)$ (square) (Ref. [13]), bulk Fe_xMn_{1-x} (solid circle) (Ref. [10]), and 15 ML $Fe_xMn_{1-x}/Cu_3Au(100)$ (open circle) as functions of Fe concentration x. All the Fe_xMn_{1-x} films are grown at RT. (b) Vertical lattice constants of 15 ML Fe films grown on 17 ML $Fe_xMn_{1-x}/Cu(100)$ (circle) (Ref. [13]) and 21 ML Fe films grown on 15 ML $Fe_xMn_{1-x}/Cu_3Au(100)$ (square). The arrows indicate the lattice constants of bulk Cu, Cu_3Au, and Fe.

The studies of $Cu_3Au(100)$ and $Cu(100)$ systems were carried out in ultrahigh vacuum chambers with the base pressure better than 2×10^{-10} torr. The substrates were prepared by cycles of sputtering and annealing.[4,11,12] Fe_xMn_{1-x} alloy films were grown by coevaporation, monitored by medium energy electron diffraction (MEED). From MEED oscillations, the deposition rate was calibrated precisely. The lateral crystalline structure was characterized by low energy electron diffraction (LEED). From the LEED-I/V curves, the average vertical lattice constant ($d_\perp$) of the film was determined by kinetic approximation.[11] Magnetic properties of the films were detected by longitudinal magneto-optical Kerr effect (MOKE).

Figure 2(a) shows the MEED oscillation curves of Fe_xMn_{1-x} alloy films grown on $Cu_3Au(100)$ at 300 K (RT). Fe_xMn_{1-x} films reveal regular oscillations. From the clear LEED patterns of $Fe_xMn_{1-x}/Cu_3Au(100)$ shown in Fig. 3, as well as the previous studies on $Fe_xMn_{1-x}/Cu(100)$,[2-9] Fe_xMn_{1-x} exhibits well-ordered crystalline structure, coherent growth, and smooth surface on both $Cu_3Au(100)$ and $Cu(100)$ over a wide range of alloy composition. Surprisingly, the larger lattice mismatch in $Fe_xMn_{1-x}/Cu_3Au(100)$ does not cause significant changes in the growth behavior. In Fig. 2(b), Fe films grown on various $Fe_xMn_{1-x}/Cu_3Au(100)$ reveal nearly the same features in MEED curves, due to the well-ordered structure and the flat surface of Fe_xMn_{1-x}. In our previous studies, Fe films on 17 ML $Fe_xMn_{1-x}/Cu(100)$ also exhibit high MEED intensity until 20-25 ML.[4,13]

Figure 4 shows the vertical lattice constants ($d_\perp$) of the Fe and Fe_xMn_{1-x} layers grown on $Cu_3Au(100)$ and $Cu(100)$. As indicated in Fig. 1, the positive lattice mismatch makes the $d_\perp$ of $Fe_xMn_{1-x}/Cu(100)$ larger than that of bulk Fe_xMn_{1-x}. The large negative lattice mismatch makes the $d_\perp$ of $Fe_xMn_{1-x}/Cu_3Au(100)$ much smaller than that of bulk Fe_xMn_{1-x}. 15 ML Fe on 17 ML $Fe_xMn_{1-x}/Cu(100)$ reveal $d_\perp \simeq 2.05$ Å with $x \leq 30\%$.[14,15] When $x > 30\%$, the 15 ML Fe

is of fcc structure ($c/a \simeq 1.0$), which is confirmed to be nonferromagnetic in our previous studies.[4,13] For 21 ML Fe films on 15 ML $Fe_xMn_{1-x}/Cu_3Au(100)$, the $d_\perp$ is deduced to be $\simeq 1.47$ Å.[16] Apparently, the epitaxial growth of Fe/Fe_xMn_{1-x} bilayers on $Cu(100)$ and $Cu_3Au(100)$ is shown to induce significant differences in $d_\perp$. Fe/Fe_xMn_{1-x} reveals similar cubic structures on both substrates, but with the more suppressed $d_\perp$ while grown on $Cu_3Au(100)$, due to the larger in-plane lattice constant.

Figure 5(a) exhibits two examples of the MOKE hysteresis loops for Fe/Fe_xMn_{1-x} bilayers on $Cu_3Au(100)$ and $Cu(100)$, after field cooling from 300 to 100–110 K along [010]. In the $Cu_3Au(100)$ system, the bias field (H_e) ranges between 200 and 300 Oe with $x = 0\% - 54\%$ at 100 K. In the $Cu(100)$ system, H_e ranges only 60–80 Oe with $x = 20\% - 30\%$ at 110 K. Due to the nonferromagnetism of fcc Fe films, no hysteresis loop can be observed with $x > 30\%$.[4,13]

For the comparison between different studies, as shown in Fig. 5(b), the interface exchange bias coupling energy $E_{ex} = H_e t_{FM} M_{FM}$ is calculated,[1] where t_{FM} and M_{FM} are the thickness and saturated magnetization of the ferromagnetic Fe layer, respectively. By substituting $M_{FM} = 2.2 \mu_B$,[17] E_{ex} is evaluated as $0.03 - 0.04$ erg/cm² for $Fe/Fe_xMn_{1-x}/Cu(100)$
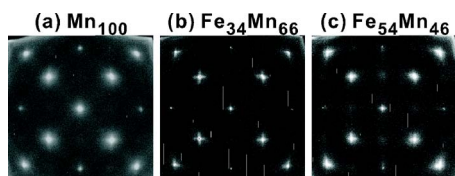

FIG. 3. (Color online) LEED patterns of the various 15 ML $Fe_xMn_{1-x}/Cu_3Au(100)$ taken at 100 K with the beam energy of 120 eV.

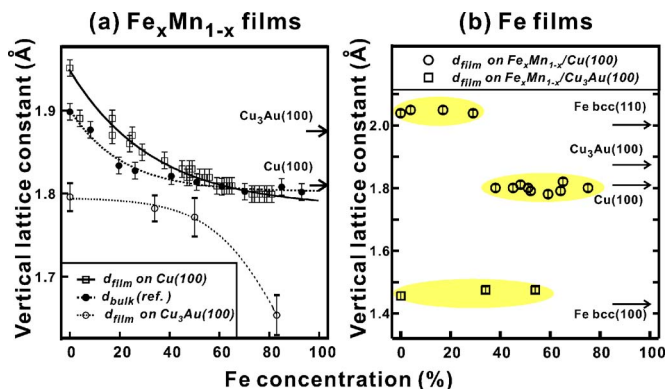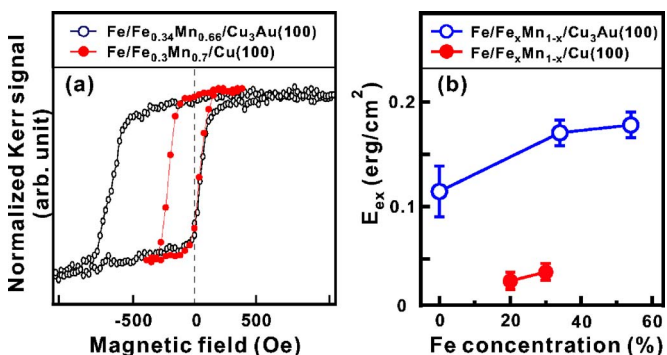FIG. 5. (Color online) (a) Normalized hysteresis loops of 21 ML Fe/15 ML $Fe_{0.34}Mn_{0.66}/Cu_3Au(100)$ and 15 ML Fe/17 ML $Fe_{0.3}Mn_{0.7}/Cu(100)$ measured at 100 and 110 K, respectively. (b) Interface exchange bias coupling energy (E_{ex}) of the Fe/Fe_xMn_{1-x} bilayers on $Cu_3Au(100)$ and $Cu(100)$ calculated from the MOKE data.

with $x=20\%-30\%$. For Fe/Fe$_x$Mn$_{1-x}$/Cu$_3$Au(100), E_{ex} $=0.12-0.18$ erg/cm^2 with $x=0\%-54\%$, which is approximately four times that of the Cu(100) system. Besides, the Fe/Fe$_x$Mn$_{1-x}$/Cu$_3$Au(100) also reveals superiority over other similar systems, e.g., Co/Fe$_x$Mn$_{1-x}$ and Ni-Fe/Fe$_x$Mn$_{1-x}$ bilayers on Cu(100). In the study by Offi *et al.*'s, a change in easy axis from the $\langle 110 \rangle$ to the $\langle 001 \rangle$ azimuth directions is observed at room temperature in a Co film coupled to a Fe$_{50}$Mn$_{50}$ film thicker than 10 ML.[2] It originates from the different orientations of the easy axis for Co film, $\langle 110 \rangle$, and the pinning direction of AFM Fe$_{50}$Mn$_{50}$, $\langle 001 \rangle$.[3] This discrepancy adds more complexity in Co/Fe$_x$Mn$_{1-x}$ exchange bias system and the bias field is shown to be small.[2] In the studies of Ni-Fe/fcc-Fe$_{50}$Mn$_{50}$ bilayers,[1,7,18,19] where the Fe$_{50}$Mn$_{50}$ is prepared in either single crystalline or (100) texture, the exchange bias coupling energy E_{ex} is evaluated as $0.04-0.07$ erg/cm^2, close to Fe/Fe$_x$Mn$_{1-x}$/Cu(100) and much smaller than Fe/Fe$_x$Mn$_{1-x}$ on Cu$_3$Au(100).

From the results of Figs. 4 and 5, the suppressed $d_\perp$ in Fe/Fe$_x$Mn$_{1-x}$ layers on Cu$_3$Au(100) could be strongly correlated to the enhanced exchange bias energy. Intuitively when the FM and AFM layers are arranged more compactly, the overlap of the electron wave functions might be also increased. Thus a stronger exchange bias coupling could be obtained. However, the detailed correlations between the $d_\perp$ in crystalline structure and the exchange bias coupling still need further theoretical studies.

In summary, this study indicates the possibility of optimizing the exchange bias by tuning the vertical lattice constants of the FM/AFM bilayers. As compared with the Cu(100) system, the larger lattice constant of Cu$_3$Au(100) results in significant suppression of the vertical lattice constants in Fe and Fe$_x$Mn$_{1-x}$ layers. The reduced vertical lattice constants in Fe/Fe$_x$Mn$_{1-x}$/Cu$_3$Au(100) enhance the interface exchange bias coupling energy E_{ex} to be $0.12-0.18$ erg/cm^2, which is approximately four times that of the Cu(100) system. The large exchange bias and well-ordered crystalline structure also suggest Fe/Fe$_x$Mn$_{1-x}$/Cu$_3$Au(100) as one of the model systems for the further studies of exchange bias coupling.

[1] J. Nogués and I. K. Schuller, J. Magn. Magn. Mater. **192**, 203 (1999).

[2] F. Offi, W. Kuch, and J. Kirschner, Phys. Rev. B **66**, 064419 (2002).

[3] W. Kuch, F. Offi, L. I. Chelaru, M. Kotsugi, K. Fukumoto, and J. Kirschner, Appl. Phys. Lett. **86**, 122504 (2005).

[4] C. C. Kuo, W. Pan, Y. C. Chen, and Minn-Tsong Lin, J. Appl. Phys. **93**, 8743 (2003).

[5] C. Won, Y. Z. Wu, H. W. Zhao, A. Scholl, A. Doran, W. Kim, T. L. Owens, X. F. Jin, and Z. Q. Qiu, Phys. Rev. B **71**, 024406 (2005).

[6] F. Matthes, A. Rzhevskii, L.-N. Tong, L. Malkinski, Z. Celinski, and C. M. Schneider, J. Appl. Phys. **93**, 6504 (2003).

[7] R. Jungblut, R. Coehoorn, M. T. Johnson, J. aan de Stegge, and A. Reinders, J. Appl. Phys. **75**, 6659 (1994).

[8] R. Thamankar, S. Bhagwat, and F. O. Schumann, Phys. Rev. B **69**, 054411 (2004).

[9] R. Thamankar, S. Bhagwat, and F. O. Schumann, Phys. Rev. B **69**, 054419 (2004).

[10] Yasuo Endoh and Yoshikazu Ishikawa, J. Phys. Soc. Jpn. **30**, 1614 (1971).

[11] W. C. Lin, L. C. Lin, T. Y. Chen, B. Y. Wang, Ker-Jar Song, and Minn-Tsong Lin, J. Appl. Phys. **97**, 10K112 (2005).

[12] B. Y. Wang, W. C. Lin, Y. W. Liao, Ker-Jar Song, and Minn-Tsong Lin, Surf. Sci. **600**, 4517 (2006).

[13] Wei Pan, W. C. Lin, N. Y. Jih, Y. C. Chen, C. H. Chuang, C. C. Kuo, and Minn-Tsong Lin, Phys. Rev. B **74**, 224430 (2006).

[14] S. Muller, P. Bayer, C. Reischl, K. Heinz, B. Feldmann, H. Zillgen, and M. Wuttig, Phys. Rev. Lett. **74**, 765 (1995).

[15] K. Kalki, D. D. Chambliss, K. E. Johnson, R. J. Wilson, and S. Chiang, Phys. Rev. B **48**, 765 (1993).

[16] M.-T. Lin, J. Shen, W. Kuch, H. Jenniches, M. Klaua, C. M. Schneider, and J. Kirschner, Phys. Rev. B **55**, 5886 (1997).

[17] K. Schwarz and D. R. Salahub, Phys. Rev. B **25**, 3427 (1982).

[18] R. Jungblut, R. Coehoorn, M. T. Johnson, Ch. Sauer, P. J. van der Zaag, A. R. Ball, Th. G. S. M. Rijks, J. aan de Stegge, and A. Reinders, J. Magn. Magn. Mater. **148**, 300 (1995).

[19] T. Lin, D. Mauri, N. Staud, C. Hwang, J. K. Howard, and G. L. Gorman, Appl. Phys. Lett. **65**, 1183 (1994).